

Electron Spin Resonance of Mn^{++} in Alkali Chlorides: Association with Vacancies and Impurities

GEORGE D. WATKINS

General Electric Research Laboratory, Schenectady, New York

(Received September 12, 1958)

The spin resonance of Mn^{++} in LiCl, NaCl, and KCl is described. In NaCl, five different spectra are observed. Designated I, II, III₁, III₂, and IV, these arise from Mn^{++} ions in five different environments. These are identified as (I) Mn^{++} ions in an aggregated or precipitated state, (II) isolated Mn^{++} ions which are not near any defect, (III₁) Mn^{++} ions with a positive ion vacancy bound in the nearest cation site, (III₂) Mn^{++} ions with a vacancy bound in the next-nearest site, and (IV) Mn^{++} ions paired off with a chemical impurity charge compensator. In LiCl and KCl only the two vacancy- Mn^{++} pairs (III₁ and III₂) are studied. In all three salts the nearest and next-nearest vacancy- Mn^{++} pairs are approximately equally stable. By studying the spectra in NaCl as the temperature is raised, the thermal dissociation of the Mn^{++} -vacancy pairs is observed, with a corresponding increase in the number of isolated Mn^{++} ions. This follows a simple mass action law giving a binding energy for the Mn^{++} -vacancy pairs of approximately 0.4 ev. An ionic point charge model of the crystalline field produced by the defects is successful in explaining several features of the spectra. However, the magnitude of the field predicted in this manner appears to be a factor of ten too low if the recent theory of Watanabe is used. This discrepancy is attributed to the role of overlap of the ion cores and/or covalency.

I. INTRODUCTION

WHEN divalent metal impurity ions are incorporated into an alkali halide lattice, they go in substitutionally for alkali ions.¹ Because of the extra positive charge of these ions, and the requirement of charge neutrality, an equal number of negatively charged defects must also be simultaneously introduced. In a pure alkali halide, the positive-ion vacancy is the easiest defect to form that satisfies this requirement. As a result, in the absence of other chemical impurities, divalent cation addition will be accompanied by the introduction of an equal number of positive-ion vacancies.¹ This is illustrated in Figs. 1 (a) and (b).

Because controlled numbers of positive-ion vacancies can be introduced in this manner, alkali halides doped with divalent cations have been studied extensively in the past in order to determine the properties of the positive-ion vacancy.¹ However, a complete interpretation of these experiments has not been possible because the importance of interaction between the divalent cations and the vacancies has not been known. A positive-ion vacancy, being a missing positive charge, can be considered as carrying an effective negative charge in the lattice. It will experience a Coulomb attraction to the extra positive charge of a divalent ion and may tend to pair off with it, as shown in Fig. 1(b). (This complex is called a simple associated pair. Complexes involving more than two defects are also possible.) The pair of Fig. 1(b) will usually contribute differently to the physical property being measured than the isolated defects of Fig. 1(a). Therefore, in order to interpret the experiments properly, it is necessary to know the degree to which association occurs. Detailed

understanding will also require knowledge of the types of complexes involved.

This problem has been given considerable attention in the literature. Theoretical estimates have been made indicating that significant association should occur.²⁻⁴ Experimental evidence of association has also been cited in ionic conductivity,¹ dielectric loss,¹ diffusion,¹ optical coloration,⁵ and nuclear resonance⁶ measurements on these or similar crystals. However, these experiments are relatively indirect and do not lend themselves to unambiguous interpretation. In some cases, the results even appear contradictory.⁷⁻⁹

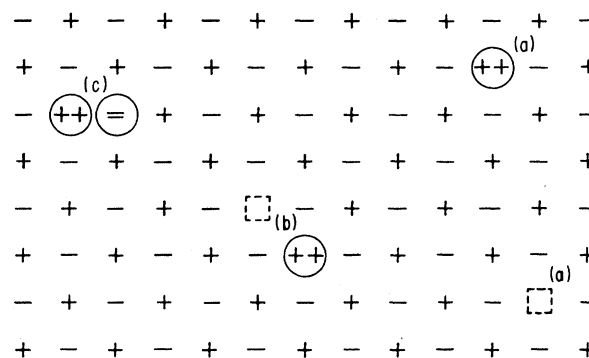


FIG. 1. Divalent ion incorporation in an alkali halide lattice. Charge compensation may arise from positive-ion vacancies either (a) separated, or (b) bound to the ion. Possible charge compensation by another chemical impurity is shown as (c).

² J. R. Reitz and J. L. Gammel, *J. Chem. Phys.* **19**, 894 (1951).

³ F. Bassani and F. G. Fumi, *Nuovo cimento* **11**, 274 (1954).

⁴ M. P. Tosi and G. Airoldi, *Nuovo cimento* **8**, 584 (1958).

⁵ Camagni, Chiarotti, Fumi, and Giulotto, *Phil. Mag.* **45**, 225 (1954).

⁶ F. Reif, *Phys. Rev.* **100**, 1597 (1955).

⁷ C. Bean, thesis, University of Illinois, 1952 (unpublished).

⁸ J. O. Thomson, thesis, University of Illinois, 1956 (unpublished).

⁹ Y. Haven, *Defects in Crystalline Solids* (The Physical Society, London, 1955), p. 261.

¹ For a review of the influence of divalent impurities in alkali halides, see F. Seitz, *Revs. Modern Phys.* **26**, 11 (1954). See also A. B. Lidiard, *Handbuch der Physik* (Springer-Verlag, Berlin, 1957), Vol. 20, p. 246.

Electron spin resonance presents a powerful tool for this study. Because the spin resonance of a paramagnetic impurity is quite sensitive to its environment, its spectrum will reflect the presence of nearby defects. If the ion is a divalent cation, such as Mn^{++} , we have a tool that allows us to look directly at the ion in question and to determine its state of association.

The first experimental use of spin resonance in this type of study was reported by Schneider and co-workers.^{10,11} They observed three distinct spectra for Mn^{++} in NaCl. They suggested that one arose from aggregated Mn^{++} , one from isolated Mn^{++} , and the third, a complex, orientation dependent spectrum, from Mn^{++} associated with a vacancy. This third spectrum was first analyzed by the author and Walker.¹² We found that it could be further divided into two different types of spectra. We identified them as arising from two types of vacancy-divalent ion pairs, one with a vacancy in the site nearest the Mn^{++} , the other with a vacancy in the next nearest site. Our analysis has since been confirmed by Schneider^{13,14} but because the spectrum identified with the nearest vacancy pair departs so strongly from axial symmetry, he has suggested that these spectra may arise from some sort of *array* of complexes rather than the simple pairs. He points out that in his measurements on quenched crystals, no evidence of thermal dissociation of the complexes is observed, which he feels also confirms this view.

In this paper, the author will attempt to show that these spectra are correctly identified with simple vacancy- Mn^{++} pairs. Arguments will be given to show that the symmetries of the spectra are indeed what one would expect for these complexes. In addition, a study of the intensity of the spectra *vs* temperature will be presented that indicates that thermal dissociation does occur, and in the manner predicted by simple association theory. Similar spectra will also be reported for Mn^{++} in LiCl and KCl.

Evidence for the thermal reorientation of the complexes is observed and is reported in the paper immediately following this one.¹⁵ Dielectric loss measurements are also reported there which directly correlate with this motion. The good quantitative agreement achieved in B also represents strong evidence for this identification.

Charge compensation for the divalent cations may also occur by the simultaneous introduction of other chemical impurities. In NaCl:Mn another spectrum will be presented which is tentatively identified as Mn^{++}

associated with a divalent negative impurity (such as O^{2-}) substituted in a nearest chlorine site.¹⁶ Evidence will be presented to suggest that another defect is also involved in the complex.

II. EXPERIMENTAL PROCEDURE

A block diagram of the spectrometer is shown in Fig. 2. It is of conventional design, using a reflection cavity and straight bolometer detection.¹⁷ The klystron is a Varian V40B and is stabilized to the sample cavity at 20 kMc/sec. The magnetic field is produced by a six-inch Varian magnet, and 15-cps modulation is achieved by additional coils around the outside of the poles. The bolometer detector is used as one arm of a dc bridge and the 15-cps signal is amplified, lock-in detected, and recorded.

For measurements up to 600°C, a noninductively wound oven is slipped over the cavity which is operated in the cylindrical TE_{011} mode and a water-cooled jacket protects the magnet pole faces. The jacket is filled with argon to prevent oxidation of the cavity. The sample is sealed off in an evacuated quartz envelope and mounted in the center of the cavity. It is attached to a quartz rod, which is brought outside the cavity and cooling jacket for rotation of the sample.

With magnetic field modulation, small with respect to a line width, the recorded signal is proportional to the derivative of the absorption. The relative number of absorbing ions in a spectrum was determined by double integration of the record with a mechanical recording planimeter. The absolute sensitivity of the spectrometer was calibrated in a straightforward manner¹⁷ by measuring the VSWR in arm 1 of the tee (see Fig. 2), the incident microwave power, the Q of the cavity and the sensitivity of the bolometer detector. With this the integrated records were used to determine the absolute number of absorbing ions.

Magnetic field measurements were made with a Numar nuclear resonance magnetometer; g values were measured by comparison of the spectra to the resonance

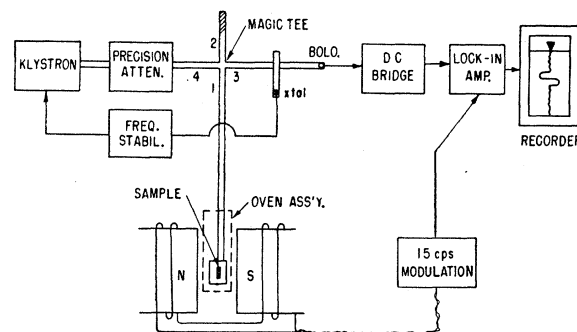


FIG. 2. Block diagram of the spectrometer.

¹⁰ E. E. Schneider and J. E. Caffyn, *Defects in Crystalline Solids* (The Physical Society, London, 1955), p. 74.

¹¹ P. A. Forrester and E. E. Schneider, *Proc. Phys. Soc. (London)* **B69**, 833 (1956).

¹² A preliminary report of this work was given by G. D. Watkins and R. M. Walker in *Bull. Am. Phys. Soc. Ser. II*, **1**, 324 (1956).

¹³ E. E. Schneider, *Arch. sci. Geneva* **10**, 120 (1957).

¹⁴ E. E. Schneider (private communication).

¹⁵ G. D. Watkins, following paper [*Phys. Rev.* **113**, 91 (1959)]. Hereafter this will be referred to as B.

¹⁶ A preliminary report of this work was given by the author in *Bull. Am. Phys. Soc. Ser. II*, **3**, 135 (1958).

¹⁷ G. Feher, *Bell System Tech. J.* **36**, 449 (1957).

of polycrystalline di-phenyl picryl hydrazil with $g=2.0036$.¹⁸

Most of the crystals studied were grown by pulling from a melt¹⁹ into which 10^{-3} – 10^{-4} mole fraction of $MnCl_2$ had been added. The melt was contained in a quartz crucible and the crystal was grown in a helium atmosphere. The starting materials were of reagent grade purity. In the case of $NaCl:Mn$, samples were also prepared from single crystals obtained from Harshaw Chemical Company. One method was to diffuse manganese into the crystal. For this a quantity of $MnCl_2$ was applied to one surface of a crystal equal to approximately 0.1-mole fraction of the crystal. The crystal was then heated at $750^\circ C$ for approximately one week in either an argon or a helium atmosphere. A second method was to use the Harshaw crystals as a high-purity source of $NaCl$ and regrow, doping in the melt.

III. THEORY OF THE SPECTRUM

The Mn^{++} spin resonance spectrum has been discussed in considerable detail in the literature.²⁰ Briefly, the Mn^{++} ion ground state is ${}^6S_{5/2}$ and is only slightly affected by its environment. Because of this, in ionic solids, its g value is isotropic and close to the free electron value, crystalline field splittings are relatively small, and relaxation times are relatively long. Mn^{55} , one hundred percent abundant, has a nuclear spin $\frac{5}{2}$ and, as a result, each electronic transition is split into six hyperfine lines. The hyperfine constant is also nearly isotropic.

The spin Hamiltonian for the ion in an external magnetic field H , and including the hyperfine interaction can be written

$$\mathcal{H} = g\beta H \cdot S + I \cdot A \cdot S. \quad (1)$$

The magnetic field for the $M \rightleftharpoons M-1$ transition is given to second order in A/H_0 by²¹

$$g\beta H (M \rightleftharpoons M-1) = h\nu_0 - Km - (A^2/2g\beta H_0) \times [I(I+1) - m^2 + m(2M-1)]. \quad (2)$$

Here ν_0 is the klystron frequency, I the nuclear spin, and m the nuclear and M the electronic azimuthal quantum numbers. K is given by

$$K^2 = A_1^2 n_1^2 + A_2^2 n_2^2 + A_3^2 n_3^2, \quad (3)$$

where the n 's are the direction cosines of the applied magnetic field to the principal axes of the hyperfine tensor. The anisotropy in A is small and has not been included in the second-order terms. In these terms A is defined as

$$A = \left[\frac{1}{3}(A_1^2 + A_2^2 + A_3^2) \right]^{1/2}.$$

In the alkali halide, the Mn^{++} substitutes for an alkali ion and the cubic crystalline environment will add a small term to the Hamiltonian:

$$\mathcal{H}_{\text{cubic}} = \frac{1}{6}a(S_x^4 + S_y^4 + S_z^4). \quad (4)$$

This gives terms which must be added to Eq. (2) and are given to first order in a by²⁰

$$\begin{aligned} g\beta\Delta H (\pm \frac{5}{2} \rightleftharpoons \pm \frac{3}{2}) &= \mp 2pa, \\ g\beta\Delta H (\pm \frac{3}{2} \rightleftharpoons \pm \frac{1}{2}) &= \pm (\frac{5}{2})pa, \\ g\beta\Delta H (\pm \frac{1}{2} \rightleftharpoons \mp \frac{1}{2}) &= 0. \end{aligned} \quad (5)$$

Here $p = 1 - 5\phi$, $\phi = n_x^2 n_y^2 + n_y^2 n_z^2 + n_z^2 n_x^2$, and n_x, n_y, n_z are the direction cosines of the magnetic field with respect to the cubic axes (x, y, z) of the crystal.

A defect near the ion destroys the cubic symmetry and a somewhat larger field splitting can occur. This additional interaction may be written^{20,22}

$$\mathcal{H}_{\text{noncubic}} = DS_1^2 + E(S_2^2 - S_3^2). \quad (6)$$

There are also terms quartic in S , but they should be small and will not be considered here. This interaction gives rise to terms which must also be added to (2) and (5) and are given to second order in D and E by

$$\begin{aligned} g\beta\Delta H (\pm \frac{5}{2} \rightleftharpoons \pm \frac{3}{2}) &= \mp 4\alpha_0 - (32\alpha_1^2 - 16\alpha_2^2)/g\beta H_0, \\ g\beta\Delta H (\pm \frac{3}{2} \rightleftharpoons \pm \frac{1}{2}) &= \mp 2\alpha_0 + (4\alpha_1^2 - 20\alpha_2^2)/g\beta H_0, \\ g\beta\Delta H (\pm \frac{1}{2} \rightleftharpoons \mp \frac{1}{2}) &= + (16\alpha_1^2 - 32\alpha_2^2)/g\beta H_0. \end{aligned} \quad (7)$$

Here,

$$\begin{aligned} 2\alpha_0 &= D(3n_1^2 - 1) + 3E(n_2^2 - n_3^2), \\ \alpha_1^2 &= D^2 n_1^2 (1 - n_1^2) + E^2 [(1 - n_1^2) - (n_2^2 - n_3^2)^2] \\ &\quad - 2DEN_1^2 (n_2^2 - n_3^2), \\ 16\alpha_2^2 &= D^2 (1 - n_1^2)^2 + E^2 [4n_1^2 + (n_2^2 - n_3^2)^2] \\ &\quad + 2DE(n_1^2 + 1)(n_2^2 - n_3^2). \end{aligned} \quad (8)$$

It is these noncubic terms that reveal the presence of a defect in close proximity to the Mn^{++} .

IV. EXPERIMENTAL RESULTS

In Fig. 3, the temperature dependence of the Mn^{++} spectrum in $NaCl$ is illustrated. At room temperature, prior to heating, a simple, broad line is observed with a width between maximum derivative points of about 130 gauss. Superposed on this line can be seen a weak complex spectrum. At $175^\circ C$ the broad line has disappeared and the intensity of the complex spectrum has increased by a factor of roughly 60. [The sensitivity in Fig. 3(a) is a factor of 20 higher than for the other temperatures, which have approximately constant sensitivity.] As the temperature is raised, most of the structure disappears, six central lines grow and at $450^\circ C$ only the six central lines remain. Upon returning

²² The distortion producing this interaction will also determine the anisotropy in the hyperfine interaction and the principal axes of Eqs. (3) and (6) will be identical.

¹⁸ Holden, Kittel, Merritt, and Yager, Phys. Rev. **77**, 147 (1950).

¹⁹ J. Czochralski, Z. physik Chem. **92**, 219 (1917).

²⁰ B. Bleaney and D. J. E. Ingram, Proc. Roy. Soc. (London) **A205**, 336 (1951).

²¹ B. Bleaney, Phil. Mag. **42**, 441 (1951).

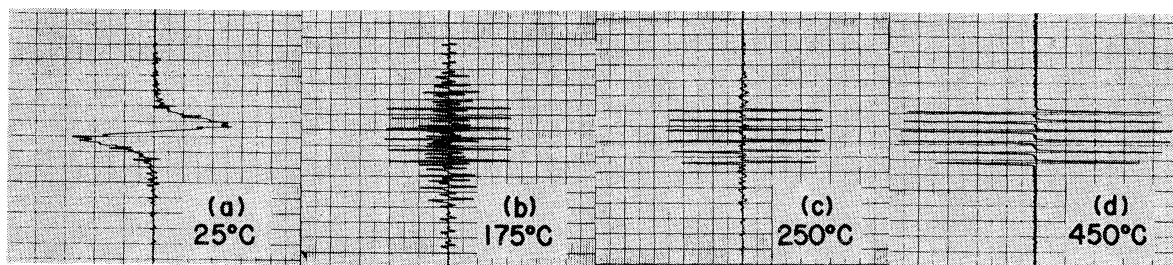


FIG. 3. Spectrum of NaCl:Mn vs temperature. The magnetic field is parallel to a cubic axis.

to room temperature, the spectrum is predominantly the complex spectrum of Fig. 3(b). This quenched-in spectrum slowly reconverts to the broad line over a period of several days. This quenching and recovery behavior has been studied in detail by Schneider *et al.*^{10,11}

Within the accuracy of measurement ($\pm 15\%$), the integrated intensity of the six lines at the highest temperature studied (600°C) is equal to that of the complex spectrum at 175°C . Similarly, the same intensity ($\mp 30\%$) is found in the broad line plus complex structure at room temperature shown in Fig. 3(a). This suggests that a constant number of Mn^{2+} ions is involved and that changes in the spectrum arise from a change of environment for these ions. This is substantiated by the comparison of the estimate of the Mn^{2+} concentration determined by chemical means with that from the resonance. In the sample used for the detailed intensity checks, the concentration estimated from the resonance was $(2.5 \mp 0.9) \times 10^{-5}$ mole fraction. The concentration estimated from emission spectrographic analysis was $(3.1 \mp 0.6) \times 10^{-5}$. Within the limits of error, this is consistent with the assumption that all of the Mn^{2+} present is accounted for in the resonance spectra.

The same general features are observed vs temperature in the LiCl and KCl samples. However, in KCl an additional strong resonance is observed which does not

convert to the other spectra as the temperature is raised. The resonance is Lorentzian in shape with a width of approximately 45 gauss between half-maximum points.¹¹ The presence of this resonance can be correlated with the existence of a white cloudiness of the crystal. This could be caused by regions in which K_4MnCl_6 had formed.²³ In the crystal as grown a sharp demarcation existed between the seed end, which was clear, and the other end, which was cloudy. In the cloudy portion, this line completely dominated the spectrum. In the clear portion, well away from the demarcation, only a very weak spectrum was observed. The sample studied was cleaved out of the clear part of the crystal close to the demarcation line. In this sample only a small amount of this additional resonance existed, and the intensity of the other spectra of interest was quite adequate for study. However, after repeated temperature cycling this resonance had grown at the expense of the other spectra. The complication introduced by this precipitated phase explains why Schneider *et al.*¹¹ found no evidence of the complex spectrum in this system.

Figure 4 shows the spectra at room temperature in quenched samples of the three salts. The dominant lines of each are made up of two distinct types of spectra. These are designated III₁ and III₂, and the

TABLE I. Spin Hamiltonian constants for Mn^{2+} spectra in alkali chlorides at 25°C .^{a,b}

System	Spectrum	g	A (10^{-4} cm^{-1})	D (10^{-4} cm^{-1})	E (10^{-4} cm^{-1})	a (10^{-4} cm^{-1})	Typical 1, 2, 3 axes	No. of such axes	Pk.-pk. deriv. width (gauss)
LiCl:Mn	III ₁	2.0018 ± 0.0002	-81.4 ± 0.4	-78 ± 4	$+47 \pm 2$...	[100], [01 $\bar{1}$], [011]	6	11.9 ± 0.3
	III ₂	2.0016 ± 0.0002	-80.8 ± 0.5	$+69 \pm 3$	≈ 0	...	[100], —	3	11.9 ± 0.3
NaCl:Mn	I	2.0043 ± 0.0006	130 ± 10
	II	2.0016 ± 0.0006	-82.3 ± 0.3	(-1)
	III ₁	2.0021 ± 0.0002	$A_1 = -82.9 \pm 0.2$ $A_2 = -82.6 \pm 0.2$	-135 ± 2	$+40.7 \pm 1.0$	(-1.3)	[100], [01 $\bar{1}$], [011]	6	9.1 ± 0.2
	III ₂	2.0022 ± 0.0004	-81.3 ± 0.4	$+131 \pm 4$	≈ 0	...	[100], —	3	9.1 ± 0.2
KCl:Mn	IV	2.0016 ± 0.0004	$A_1 = -78.7 \pm 0.4$ $A_2 = A_3 = -79.6 \pm 0.4$	-512 ± 11	$+19 \pm 2$...	rotate cubic axes about [100] (2 axis) by $1.3 \pm 0.1^\circ$	12	8.4 ± 0.5
	III ₁	2.0018 ± 0.0002	-81.8 ± 1.0	-198 ± 5	$+41 \pm 2$...	[100], [01 $\bar{1}$], [011]	6	8.6 ± 0.4
	III ₂	2.0017 ± 0.0002	-81.7 ± 1.0	$+174 \pm 4$	0 ± 3	...	[100], —	3	8.6 ± 0.4

^a g has been determined with respect to 2.0036 for DPPH. The indicated errors do not include the uncertainty in the absolute value for DPPH, which is ± 0.0002 (see reference 18).

^b A has been assumed to be negative.

²³ This possibility was pointed out to the author by P. D. Johnson of this laboratory.

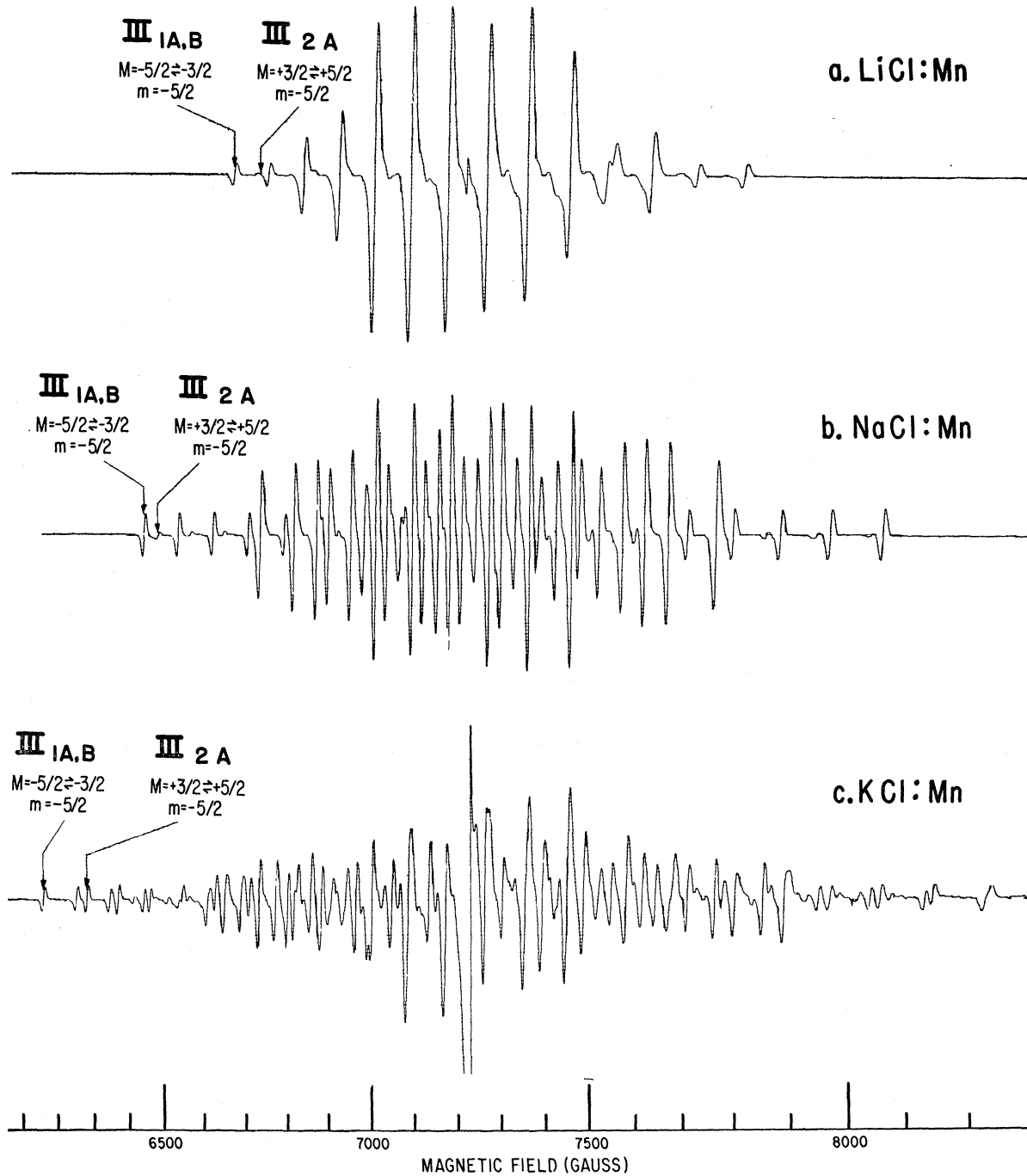


FIG. 4. Room-temperature spectrum in quenched crystals of (a) LiCl:Mn, (b) NaCl:Mn, and (c) KCl:Mn. The magnetic field is parallel to a cubic axis.

spin Hamiltonian constants are given in Table I.^{24,*} (A has been assumed to be negative since this is the sign

²⁴ The Roman numeral designation of the spectra used in this paper was chosen so as to conform with that used by Schneider.¹⁸

* Note added in proof.—Morigaki, Fujimoto, and Itoh [J. Phys. Soc. (Japan) 13, 1174 (1958)] have reported a study of spectrum III₁ in aqueous grown NaCl. Their results are in agreement with

found in all cases which have been investigated.²⁵ Columns 8 and 9 give the principal axes of the interac-

ours, the apparent difference in D and E resulting from a different choice of principal axes.

²⁵ See, for example, K. D. Bowers and J. Owen, *Reports on Progress in Physics* (The Physical Society, London, 1955), Vol. 18, p. 304.

tions. These spectra are produced by distortions from the normal cubic environment, and all equivalent distortions will occur with equal probability. This means that each spectrum is comprised of a superposition of several spectra which are identical except that they have different sets of equivalent principal axes.

Spectrum III₁ has six equally probable sets of principal axes. Each set is made up of one of the three cubic axes (the 1 axis) and one of the two possible sets of [110] axes at right angles. For instance, ([100], [011], [011]) makes one such set. Six sets with five electronic transitions, each split into six lines by the hyperfine interaction, gives 180 lines to the spectrum for an arbitrary orientation of the crystal with respect to the magnetic field. The spectrum was studied by rotating a crystal both around a [100] axis and a [110] axis perpendicular to the magnetic field. (Around these axes, the number of lines is reduced to 120.) In LiCl, the spread of the spectrum is greatest with H_z parallel to a [110] direction. Convention would normally dictate that this be labeled the 1 axis. However, for clarity in comparison with the other salts, the 1 axis is still taken as a [100] direction in Table I.

Spectrum III₂ is essentially axially symmetric around one of the three cubic axes and therefore gives rise to 90 lines. In NaCl and LiCl the intensity in this spectrum was approximately 15% that in spectrum III₁ and the lines were clearly separable only in a narrow angular range around H_z parallel to a cubic axis. Hence, a slight asymmetry (i.e., $E > 0$) could exist. In KCl, however, spectrum III₂ is 50% more intense than spectrum III₁, and E is found to be zero within the accuracy of the analysis. As a result, axial symmetry is assumed for LiCl and NaCl.

Discrepancies between the experimental spectra and those predicted by Eq. (6) indicate the existence of small terms quartic in S . However, because of the complexity of the spectra, it was not possible to determine the exact nature of them. The indicated errors in D and E result mainly from the failure to include these terms. In NaCl, the quartic terms of Eq. (4) were included for spectrum III₁ and the maximum discrepancy between the calculated and observed position of any line in the spectrum could be reduced from ∓ 4 gauss to ∓ 2 gauss with a cubic field constant $a = -1.3 \times 10^{-4} \text{ cm}^{-1}$. This indicates that quartic terms still remain, with the symmetry of D and E , which are of the same order of magnitude. The value of a is indicated in parentheses because it may not have been separated properly from the remaining quartic terms.

The remaining spectra (I, II, IV) have been analyzed only in NaCl. The six-line spectrum dominant at elevated temperatures is designated spectrum II. Except for small intensity variations, this spectrum is independent of the orientation of the crystal in the magnetic field. The intensity of the spectrum is weak at room temperature and it was not possible to separate it

from the other spectra at this temperature. As a result, the room-temperature value of A in Table I was estimated by measuring A as the temperature was lowered and extrapolating to room temperature. Since no facility was available for measuring the klystron frequency accurately, the g value was measured at 150°C relative to that of spectrum III₁. The relative intensity of spectrum II increases in samples of low Mn^{++} concentration and the study was made in low concentration samples.

There is an asymmetric envelope to the six lines of spectrum II at elevated temperatures [see Fig. 3(d)]. Each line is the superposition of the five electronic transitions, and second-order terms in the hyperfine interaction will tend to destroy their exact superposition, the outside lines being broadened the most. This effect alone would cause a symmetrical envelope. Including a cubic field interaction with $a \approx -1 \times 10^{-4} \text{ cm}^{-1}$ could produce the asymmetry observed. The behavior of this envelope as the crystal is rotated also agrees closely with this model; the asymmetry goes through zero and reverses as the crystal is rotated from the magnetic field along a [100] axis, to along a [110] axis. The value of a is given in parentheses in the table because the cubic field splittings are not resolved, and one cannot rule out other explanations for the asymmetry.

The broad line of Fig. 3(a) is labeled spectrum I. The results agree approximately with those of Schneider,^{10,11} Low,²⁶ and Oshima *et al.*²⁷ in solution and melt-grown crystals. The g value given in Table I is slightly lower and closer to the free-electron value than that measured by these other workers at 3 cm.

Spectrum IV is a complex spectrum, observed in NaCl, which has an order of magnitude lower intensity (see Fig. 5). It was present at approximately the same intensity in almost all crystals, whether melt- or diffusion-doped. The principal axes are those obtained by rotating $1.3^\circ \mp 0.1^\circ$ about the cubic axis designated the 2 axis. There are 12 sets of axes, giving rise to 360 lines.

In diffusion-doped crystals, a sharp concentration gradient existed, the Mn^{++} concentration being down to less than 10^{-7} , $\frac{1}{2}$ cm from the surface. By sectioning the crystal the spectra could be studied at varying Mn^{++} concentrations. Spectrum IV grows first, saturating at a concentration usually around $(1-3) \times 10^{-6}$. Additional Mn^{++} gives rise to spectra I through III, with no increase in the intensity of spectrum IV. It appears that there exist in the crystal a fixed number of sites to which a Mn^{++} is strongly attracted. These sites are filled first in the doping. The fact that a few crystals did not show spectrum IV suggests that the site may be a chemical impurity. Because of this initial selective population, low-concentration samples contained pre-

²⁶ W. Low, Proc. Phys. Soc. (London) **B69**, 837 (1956).

²⁷ Oshima, Abe, Nagano, and Nagusa, J. Chem. Phys. **23**, 1721 (1955).

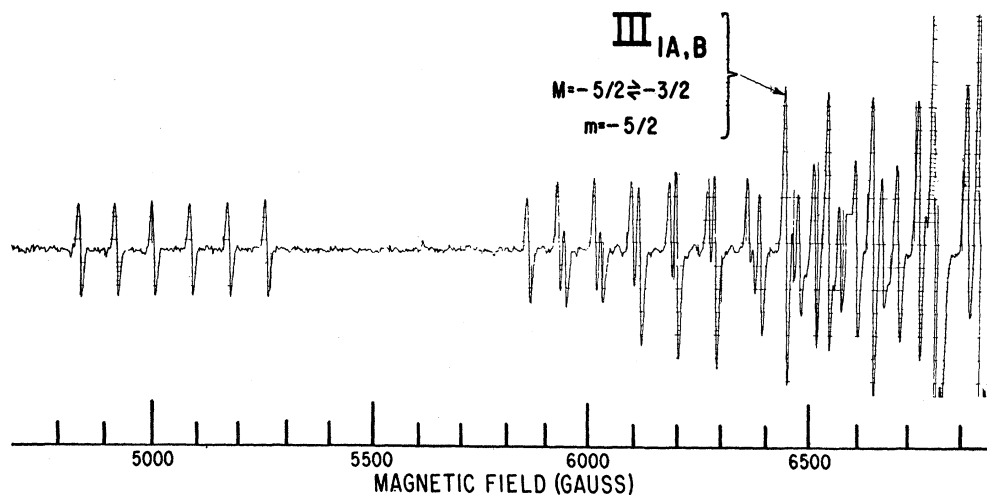


Fig. 5. NaCl:Mn spectrum at increased sensitivity showing part of spectrum IV. The low-field spectrum III_1 satellite is indicated for reference. All of the lines observed to the low-field side of the indicated III_1 satellite are part of spectrum IV.

dominantly spectrum IV. (In Fig. 5, the relative increase in spectrum IV over spectrum III_1 compared to Fig. 4 is primarily because the sample of Fig. 5 has a lower Mn^{++} concentration.)

In NaCl, the individual satellite lines of spectra III_1 and III_2 broaden abruptly in a narrow temperature range (see Fig. 6). Similar effects occur in LiCl and KCl at slightly different temperatures. A detailed study of this effect is given in B. It is concluded there that the fine-structure splittings D and E are being averaged out due to a thermally induced motion of the defects producing the splittings.

In spectrum IV, there is evidence of limited motion. In approximately the same temperature range as for the broadening of the spectra III_1 and III_2 satellites, the asymmetry, as measured by E , is motionally averaged out. D , however, is not averaged out to at least $400^\circ C$. The intensity in spectrum IV appears roughly constant up to approximately $400^\circ C$, at which point the spectrum disappears. It has not been determined whether the lines broaden as they disappear or not. On recooling, the spectrum reappears.

In addition to the spectra I-IV in NaCl, which are clearly identifiable with Mn^{++} , another very broad line, approximately 850 gauss wide, between half-maximum points was sometimes observed. The origin of this is not understood. In the sample for which most of the detailed intensity measurements were made, the integrated intensity of this line was approximately equal to the total intensity of the Mn^{++} spectra I through IV, even though the derivative presentation made it practically unobservable. The close agreement between the chemical and resonance estimates (excluding this broad line) make it unlikely that it is due to manganese. The overlap of errors is sufficiently great, however, to accommodate the possibility. At least up to $450^\circ C$ the line appears to be roughly constant in shape and area.

To the degree that its intensity is constant, we can ignore its participation in the detailed balance between spectra I-IV vs temperature.

V. MODELS FOR THE SPECTRA

A. Spectrum I

Spectrum I of NaCl has been considered in some detail by Schneider *et al.*^{10,11} They point out that the absence of resolved hyperfine structure and the relatively narrow Lorentzian line shape indicates the existence of strong exchange narrowing. They therefore

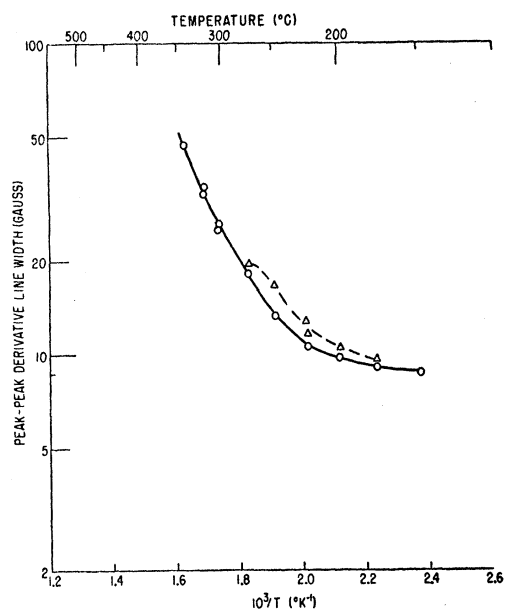


Fig. 6. Dependence of line width on temperature in NaCl:Mn. The circled points are for the $M = -\frac{5}{2} \rightarrow -\frac{3}{2}$, $m = -\frac{5}{2}$ multiplet of spectrum III_1 ; the triangled points are for the $M = +\frac{3}{2} \rightarrow +\frac{5}{2}$, $m = -\frac{5}{2}$ multiplet of spectrum III_2 [see Fig. 4(b)].

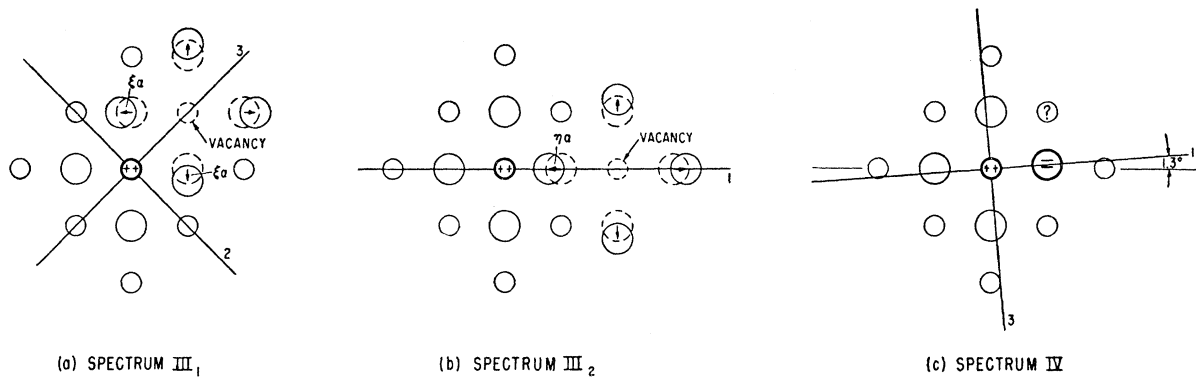


FIG. 7. Models of the spectra. The large circles are the anions, the small circles, the cations. The displacements of the anions around the vacancy are shown. There is also an inward displacement of the anions surrounding the divalent ion which is not shown. This displacement maintains the cubic symmetry and does not contribute to the fine structure splittings.

conclude that the manganese ions are in close proximity to each other, aggregated at or near internal boundaries or dislocations. An additional verification is as follows: We have observed that quenched crystals with no spectrum I are much softer (blend upon cleaving) than those which have predominantly spectrum I. This suggests that the crystal is "precipitation hardened" by the aggregated manganese. Heating the crystal "dissolves" the manganese ions into the lattice and the crystal again becomes "soft." (Similar heat treatment effects have been observed on the hardness of pure LiF crystals by Johnston and Gilman.²⁸ They conclude also that the effects are due to precipitation hardening by impurities.) The disappearance of spectrum I as the temperature is raised is interpreted as arising from the dissolving of the aggregated Mn^{++} into the solid. The temperature range in which this occurs agrees with the solubility estimates of Haven⁹ from ionic conductivity measurements on this system.

The absence of resolved hyperfine structure and crystal field splittings arises from the exchange narrowing. However, these interactions are still present and shift the average center of gravity of the spectrum to lower field. From Eqs. (2), (7), and (8) we can estimate a shift of

$$\langle \Delta H \rangle_{Av} \approx -[0.63D^2 + (5/12)A^2/g^2\beta^2H_0]. \quad (9)$$

This explains the different apparent g value reported here (2.0043) from those reported at 3 $cm^{13,26,27}$ (2.010–2.015). Applying Eq. (9) with $A \approx -82 \times 10^{-4} cm^{-1}$, we can estimate from the measurements at the two different wavelengths an rms value for D in the precipitated state of ≈ 0.03 – $0.04 cm^{-1}$, a reasonable value.

The true g value, without the shift of Eq. (9), is therefore 2.001 ∓ 0.001 , in good agreement with the other spectra.

²⁸ W. G. Johnston and J. J. Gilman, General Electric Research Laboratory (private communication).

B. Spectrum II

Spectrum II is caused by manganese ions perturbed only by cubic fields. The spectrum therefore results from isolated Mn^{++} ions, with no defect nearby. The increase in its intensity as the temperature is raised is due to an increase in the number of isolated ions. (The possibility that there is a defect nearby, but that its motion is so rapid that its effect is averaged out, is considered in Sec. VII and can be ruled out over the temperature range studied.)

C. Spectrum III₁

We believe that spectrum III₁ is due to Mn^{++} with a positive ion vacancy in the nearest cation site as shown in Fig. 7(a). The symmetry of the splittings due to the crystal field is consistent with this interpretation. In addition, the relative values of D and E can be shown to be consistent with a simple ionic point charge model for the effective crystalline field acting on the Mn^{++} ion, as follows: Terms quadratic in S arise from terms in the Hamiltonian for d electrons which are quadratic in r , the position coordinate. In a simple ionic model, this part of the Hamiltonian is given by $\sum_i [-|e|V(r_i)]$, where $V(r_i)$ is the electrostatic potential at the i th electron produced by all of the surrounding ions. The quadratic terms, zero in cubic symmetry, arise both from the missing positive charge of the vacancy and from the electronic and displacement polarization of the ions surrounding the vacancy. Because the polarization falls off as r^{-3} from the vacancy, and because the contribution to the quadratic terms from a displaced charge also falls off as r^{-3} , a reasonable approximation for the contribution of the polarization is to consider only the two chlorine ions adjacent to both vacancy and Mn^{++} . The polarization of these ions can be represented by a fractional displacement ξ as shown in Fig. 7(a). Considering the vacancy as a single negative charge $\sqrt{2}a$ away and the chlorine ions as single negative charges displaced a distance ξa as shown, the quadratic

part of the potential may be written

$$V = D'x_1^2 + E'(x_2^2 - x_3^2) - \frac{1}{3}D'r^2, \quad (10)$$

where

$$\begin{aligned} D' &= 3|e|/8\sqrt{2}a^3, \\ E' &= (|e|/a^3)[(3/8\sqrt{2}) - 3\xi]. \end{aligned} \quad (11)$$

D and E should be roughly proportional to D' and E' , so that in order to explain the relative values of D and E for NaCl (Table I), $\xi=0.115$. This represents an induced dipole $0.115 ae$, which is not unreasonable for the combined electronic and displacement polarization. Bassani and Fumi³ have calculated that in NaCl the displacement of the ions alone is $0.083 a$.

The agreement is better than one would expect. However, the calculation does explain the large asymmetry in the crystal field splittings and shows that it arises primarily from the distortion of the nearest neighbor chlorine ions surrounding the Mn^{++} .²⁹⁻³¹

A calculation of the relation between D and D' , etc., has recently been made by Watanabe.³² His result states that

$$D = -9.90\Delta^2 \times 10^{-10} + 3.62M'\Delta \times 10^{-5} \text{ cm}^{-1}, \quad (12)$$

where

$$\Delta = -eD'\langle r^2 \rangle / 3hc. \quad (13)$$

Here M' is a measure of the spin-spin interaction between an electron in the $3d$ and $4s$ orbital states, $\langle r^2 \rangle$ is the average value of r^2 for a $3d$ orbit. M' is difficult to estimate because it depends strongly upon the overlap of the $3d$ and $4s$ wave functions, but Watanabe suggests $0.1-0.3 \text{ cm}^{-1}$ as a reasonable value. Taking $M'=0.2 \text{ cm}^{-1}$, and $\langle r^2 \rangle = 0.4 \times 10^{-16}$ as determined from Hartree functions,³³ $D = -14 \times 10^{-4} \text{ cm}^{-1}$ for NaCl. The sign is correct, but the magnitude is a factor of ten too low. The main source of error may not be in Watanabe's result but rather in the simple ionic point charge approximation to D' . Because of the strong exchange forces due to overlap with the charge clouds of its neighbors, the effective potential for the Mn^{++} ion produced by displacements of its neighbors may be

²⁹ Experimentally we cannot distinguish whether the vacancy is along the 2 or 3 axis. The preceding arguments suggest that it is along the 3 axis as shown in Fig. 7(a).

³⁰ Additional indirect evidence that this model for spectrum III₁ is reasonable is available from the double resonance measurements by Feher³¹ on the F center in KCl. He measured the nuclear quadrupole coupling at the chlorine ion nearest to the F center and found the same set of axes and a large asymmetry with $D'/E' = -1.7$. (The nuclear quadrupole coupling also measures the quadratic part of the potential, in this case at the position of the nucleus.) The negative-ion vacancy (which is the center of the F center) occupies the same position relative to the chlorine nucleus studied, as does the positive-ion vacancy to that of the Mn^{++} ion, and there should be a high degree of similarity between the two. Because of the additional anisotropy in the magnetic hyperfine interaction, Feher can distinguish between the 2 and 3 axes, and the negative value for D'/E' is consistent with the identification here of the vacancy along the 3 axis.

³¹ G. Feher, Phys. Rev. **105**, 1122 (1957).

³² H. Watanabe, Progr. Theoret. Phys. Japan **18**, 405 (1957).

³³ D. R. Hartree, Proc. Cambridge Phil. Soc. **51**, 126 (1955).

considerably in excess of that predicted by the motion of hypothetical charges centered on the nuclei. Also covalent bond formation has been ignored. (It will be shown in Sec. VI that a significant amount of covalency does exist for the manganese ion.) It is possible that the crystal field splittings are very sensitive to a small amount of covalency in much the same way that nuclear quadrupole coupling constants often are.³⁴

Although the point-charge model predicts field splittings a factor of ten too low, the preceding arguments concerning the *ratio* of D to E may still be considered to have significance. In fact, we may obtain an indication of the importance of overlap and covalent effects by comparison of the ratio D/E observed in NaCl with that in the other two alkali chlorides. In LiCl, for instance, because of the larger ratio of anion to cation radii, the Mn^{++} will have less overlap with its Li^+ neighbors. As a result, a missing Li^+ will not affect the Mn^{++} as much and the spectrum will be determined more by the polarization of its six nearest neighbors. From Eq. (11), this means a lower magnitude of D'/E' (still negative), which is observed. The opposite will be true in KCl, where significant overlap with K^+ neighbors can occur. This also agrees with the observed spectrum. As a result, we may conclude that these effects are important.

The rapid increase in line width could be caused by the diffusion of the vacancy from one bound site to another. Each time the vacancy jumps the spectrum will change, giving rise to a lifetime broadening of the individual lines. It is well known that the vacancy is highly mobile¹ and the line broadening in itself must be considered strong evidence that a vacancy is involved in the complex. This motion will be considered in detail in paper B.

Finally, the simple vacancy- Mn^{++} complex is expected to exist and to be the most prevalent complex. It is natural then to identify it with spectrum III₁, which satisfies the necessary requirements.

D. Spectrum III₂

Spectrum III₂ is identified as arising from Mn^{++} ions which are bound to a vacancy in the next-nearest possible position [see Fig. 7(b)]. Because the vacancy is in a cube direction from the Mn^{++} , both its direct effect and the polarization give rise to axial symmetry around this direction. Again considering only the displacement of the chloride ion adjacent to both vacancy and Mn^{++} ion plus the direct effect of the vacancy, the simple ionic approximation gives

$$\begin{aligned} D' &= -(|e|/16a^3)(3+72\eta), \\ E' &= 0. \end{aligned} \quad (14)$$

The 1 axis is along the cubic axis toward the vacancy, and ηa is the displacement of the bridging chloride

³⁴ Honig, Mandel, Stitch, and Townes, Phys. Rev. **96**, 638 (1954).

TABLE II. Relative stabilities of nearest neighbor (III₁) and next-nearest neighbor (III₂) vacancy complexes.

	n_1/n_2 (25°C spectra)	$E_1 - E_2$ (spectra) ev	$E_1 - E_2$ (Sr ⁺⁺ theory) ^a ev
LiCl	7.4	+0.034	...
NaCl	7.5	+0.034	+0.02
KCl	0.65	-0.029	-0.11

^a F. Bassani and F. G. Fumi, *Nuovo cimento* **11**, 274 (1954); M. P. Tosi and G. Airoldi, *Nuovo cimento* **8**, 584 (1958).

ion produced by the vacancy as shown in Fig. 7(b). Using $\eta=0.048$ as calculated by Tosi and Airoldi⁴ for NaCl:Sr⁺⁺, Eqs. (12) and (13) give, for NaCl, $D = +21 \times 10^{-4} \text{ cm}^{-1}$. As in spectrum III₁, the sign is correct but the magnitude is almost a factor of ten too low.

The multiplets of spectrum III₂ also broaden as the temperature is raised, as is shown in Fig. 6. This suggests that a vacancy is involved in this complex too. Finally, the model is the simplest complex that satisfies the symmetry of the spectrum.

The ratio of the number of nearest to next-nearest complexes at room temperature, as determined from relative intensities is given in Table II. Assuming detailed balance between the two complexes and the same vibrational frequencies for the vacancy in each, this ratio is given by

$$n_1/n_2 = (12/6) \exp[(E_1 - E_2)/kT], \quad (15)$$

where 12/6 is the ratio of available nearest to next-nearest sites, and E_1 and E_2 are the binding energies of the complexes. The values of $E_1 - E_2$ required to give the room temperature ratios are also given in Table II. The difference in binding energies of the two complexes is small, and in KCl the next-nearest site is actually the more stable.

It is surprising that the next-nearest site, a factor $\sqrt{2}$ farther away from the Mn⁺⁺ than the nearest site, could be this stable. However, Tosi and Airoldi⁴ have calculated the binding energy of a vacancy to Sr⁺⁺ in NaCl and KCl for the next-nearest site. Comparing their values to those calculated by Bassani and Fumi³ for the same ion in a nearest vacancy complex, they find that the energies are indeed comparable. In fact, their calculations predict that the next-nearest site is the more stable in KCl while the nearest is the more stable in NaCl. Although these calculations were performed for Sr⁺⁺, it seems reasonable that they are representative of any divalent ion, and this agreement must be considered additional evidence in support of the identification of these spectra.

E. Spectrum IV

A model which can explain the properties of spectrum IV is shown in Fig. 7(c). In this model, one of the six nearest chloride ions has been replaced by a doubly negatively charged impurity ion (such as O²⁻, S²⁻, etc.).

Because the impurity ion carries an extra negative charge and is next to the Mn⁺⁺ ion, a large Coulombic binding energy is expected. This explains why these sites are populated first in the doping. The close proximity of the extra negative charge also explains the large crystal field splittings. The low-temperature width of the individual resonance multiplets is approximately 10% less than those in spectra II, III₁, and III₂ (see Table I). The width originates from hyperfine interaction with the neighboring chlorine nuclei (see Sec. VI) and the replacement of one ion by a magnetically inert group VI ion would reduce the width by about this amount. The failure to detect motional averaging of D up to 400°C is consistent with a relatively immobile substitutional impurity.

The origin of the asymmetry is less clear. It was suggested in a preliminary report¹⁶ that the asymmetry might arise from a Jahn-Teller³⁵ distortion of the double negative ion. (This could arise as a result of partial electron transfer away from the X²⁻ leaving a partial hole whose orbital degeneracy could be lifted by the distortion.³⁶) However, the barrier for motion for such a complex from one distorted position to another would probably be only a fraction of the Jahn-Teller energy, and therefore probably $\lesssim 0.1$ ev. The temperature range at which E is averaged out indicates, if one assumes normal vibrational frequencies, a barrier energy ~ 0.6 ev. As a result, it is now believed that another defect is probably present, perhaps in the cation site marked with a question mark in Fig. 7(c). A positive ion vacancy suggests itself, but it is not clear why it should be so strongly bound. (There is evidence that it is still bound at 400°C.) A more probable defect is a small substitutional impurity, bound to the double minus ion primarily by covalent forces. One possibility is (OH)⁻, with the oxygen in the anion site and the hydrogen in the cation site. The smallness of the hydrogen would allow it to diffuse around the oxygen with essentially the same mobility as the positive ion vacancy it occupies.

Using the simple point-charge model of a single extra negative charge located at the position of a nearest chlorine site, the value of D' in Eq. (10) is $-3|e|/2a^3$. This value, with Eq. (12), gives $D = +67 \times 10^{-4} \text{ cm}^{-1}$, which is of the wrong sign and an order of magnitude too low. However, in Watanabe's equation there is a quadratic term which will reverse the sign if D' is larger. Solving Eq. (12) for the required D' , we find that it must be a factor of eleven larger than that given by the point charge model. A factor of this size has also been required to explain the splittings observed in spectra III₁ and III₂. As a result, if one estimates that the crystalline potential is approximately ten times that given by the simple point charge model, the field splittings of all

³⁵ H. A. Jahn and E. Teller, *Proc. Roy. Soc. (London)* **A161**, 220 (1937).

³⁶ The origin of the degeneracy was pointed out to the author by Professor Morrel H. Cohen, University of Chicago.

three spectra agree with those predicted by the models of Fig. 7. The factor of ten may arise from the effect of overlap and covalency.

VI. LINE WIDTH

At room temperature the individual resonance multiplets of spectra III_1 and III_2 are approximately Gaussian in shape with the peak-peak derivative widths shown in Table I. Dipolar fields from the nuclear magnetic moments of neighbors can be shown using Van Vleck's formula³⁷ to contribute only about one gauss or less. The widths are insensitive to the physical perfection of the crystal and of the Mn^{++} concentration over a wide range. As a result, the broadening can be considered to be due to hyperfine interaction with the neighboring chlorine nuclei. There are two isotopes of chlorine each with spin $\frac{3}{2}$ giving such a large number of hyperfine arrangements that they are not resolved.

The magnitude of the widths is reasonable for this mechanism as can be seen by comparison with results of Tinkham³⁸ for Mn^{++} in ZnF_2 . Here the hyperfine interaction with the six fluorine neighbors was resolved. Following the approach of Van Vleck,³⁹ Stevens,⁴⁰ and Owen.⁴¹ Tinkham considered the smeared-out magnetic orbitals as linear combinations of the $3d$ wave functions on the central manganese ion and a small amount of σ and π orbitals around the six attached ions. In order to account for the observed structure, he concluded that each of the five magnetic electrons spends approximately 6% of its time in $n=2$ orbitals on the neighboring F^- ions. A similar analysis here gives the identical result for $n=3$ orbitals on the Cl^- ions. The σ orbitals are assumed to have 20% $3s$ character, for which Hartree functions⁴² give a probability density at the nucleus of $|\psi_{3s}(0)|^2 = 70 \times 10^{-24} \text{ cm}^{-3}$.

VII. VACANCY- Mn^{++} BINDING ENERGY IN NaCl

Study of the relative integrated intensities of spectra II, III_1 , and III_2 vs temperature should allow the determination of the binding energy of the vacancy to the manganese. This assumes that spectrum II is correctly interpreted as arising from isolated Mn^{++} ions. Another interpretation of spectrum II must first be ruled out, namely, whether it could arise from spectra III_1 and III_2 , which have been motionally narrowed due to the diffusional motion of the attached positive-ion vacancy.⁴³ This would occur in three distinct steps. First, there might be an apparent increase of the six central lines due to the averaging of the second and

higher order shifts of the $M = +\frac{1}{2} \rightleftharpoons -\frac{1}{2}$ transitions. This would occur in the same temperature range as does the onset of broadening for the $M = \pm\frac{5}{2} \rightleftharpoons \pm\frac{3}{2}$ satellite studied (Fig. 6). However, with the magnetic field parallel to a 100 direction, these shifts are at their minimum and such an effect will be small and can be neglected. The next two steps would occur when first the $M = \pm\frac{3}{2} \rightleftharpoons \pm\frac{1}{2}$ and then the $M = \pm\frac{5}{2} \rightleftharpoons \pm\frac{3}{2}$ first-order shifts are averaged out. These transitions will not be mistaken for spectrum II until they have been narrowed to the approximate width of the spectrum II lines. The point at which this will occur can be estimated by reference to the work of Gutowsky, McCall, and Slichter.⁴⁴ As the jump time τ becomes short, the spectrum that they studied, originally made up of two lines separated by $2\Delta f$, is replaced by a single central line whose width is given by the original unbroadened line width of the satellites plus a Lorentz broadening with $1/T_2 = 2\pi^2\Delta f^2\tau$. This can be derived from Eq. (41) of their paper. Solving for a T_2 broadening equal to the spectrum II width, and using for the present case Δf^2 averaged over all of the nearest and next-nearest sites, $\tau = 2 \times 10^{-11}$ second for the $M = \pm\frac{3}{2} \rightleftharpoons \pm\frac{1}{2}$ transition. The $M = \pm\frac{5}{2} \rightleftharpoons \pm\frac{3}{2}$ requires τ a factor of four shorter. From Eq. (7) of reference B, a temperature of 750°C is required for $\tau \approx 2 \times 10^{-11}$ sec. We conclude that this is not important in the temperature range studied (up to 600°C), and that spectrum II is correctly identified as arising from isolated Mn^{++} ions.

Unfortunately, because of the broadening of the spectrum III_1 and III_2 satellites, it is not possible to use the resonance to determine the number of Mn^{++} ions in these complexes above $\approx 300^\circ\text{C}$. However, the intensity of the central six lines has been measured up to 600°C. If we assume that a constant number of Mn^{++} ions are divided between spectra II, III_1 , and III_2 (I does not exist at these temperatures and IV is negligible), the increase in spectrum II will be accompanied by a corresponding decrease in spectra III_1 and III_2 . Therefore, by measuring the total intensity at 200°C, for example, the relative number of associated and unassociated Mn^{++} ions can be computed from the intensity of the central six lines vs temperature. Defining p as the percentage of Mn^{++} ions associated with a vacancy (nearest and next nearest), and $(1-p)$ the percentage that are isolated, the intensities of the various spectra are given by

$$I_{\text{central}} = [(1-p) + (9/35)p]I_0, \quad I_{III_1+III_2} = pI_0. \quad (16)$$

The term containing 9/35 represents the intensity of the $M = +\frac{1}{2} \rightleftharpoons -\frac{1}{2}$ transitions of spectra III_1 and III_2 which also contribute to the central six lines. (The almost identical values of g and A for the three spectra and the small second-order shifts for the central components of spectra III_1 and III_2 allow simple addition of their intensities.)

⁴⁴ Gutowsky, McCall, and Slichter, J. Chem. Phys. **21**, 290 (1953).

³⁷ J. H. Van Vleck, Phys. Rev. **74**, 1168 (1948).

³⁸ M. Tinkham, Proc. Roy. Soc. (London) **A236**, 535 (1956).

³⁹ J. H. Van Vleck, J. Chem. Phys. **3**, 807 (1935).

⁴⁰ K. W. H. Stevens, Proc. Roy. Soc. (London) **A219**, 542 (1953).

⁴¹ J. Owen, Proc. Roy. Soc. (London) **A227**, 183 (1955); Discussions Faraday Soc. **19**, 127 (1955).

⁴² D. R. Hartree and W. Hartree, Proc. Roy. Soc. (London) **A156**, 45 (1936).

⁴³ The arguments given here are abbreviated. For a detailed discussion of the effect of vacancy motion on the spectra, see B.

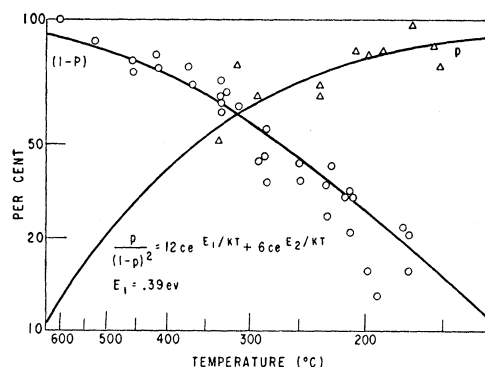


FIG. 8. Degree of association *vs* temperature for Mn^{++} in NaCl. The solid line is a simple mass action law where p gives the percentage of Mn^{++} ions associated with vacancies. The triangled points are estimates of p from the intensity of spectra III₁ and III₂. The circled points are estimates of $(1-p)$ from the central six lines.

The results of a detailed analysis in one crystal of NaCl:Mn using Eq. (16) is shown in Fig. 8. The curve is a simple mass action law with a binding energy for the nearest vacancy pair $E_1=0.39$ ev. The mole fraction c was taken as 60 ppm, and E_1-E_2 was taken as $+0.034$ ev (see Table II).

Although the scatter of points is rather large, the data indicates that the complexes are thermally dissociating and that a simple mass action law can describe the process. The value of the binding energy is considered tentative for two reasons: (1) Emission spectrographic analysis has revealed that 29 ± 6 ppm of Ca^{++} exist in the crystal in addition to the 31 ± 6 ppm Mn^{++} . The Ca^{++} apparently was an impurity present in the NaCl starting material. Since Ca^{++} ions are also competing for vacancies, this could upset the detailed balance between the Mn^{++} and its vacancies. If the binding energy for Ca^{++} is the same as that for Mn^{++} , the analysis is valid so long as the combined concentration is used in the mass action formula. This was done to arrive at $E_1=0.39$ ev. Although one expects essentially the same binding energy for the two, Ca^{++} has been reported to behave curiously,⁷⁻⁹ and this may introduce some error. (2) The sample also exhibited a broad unidentified resonance, described in Sec. IV, of intensity about equal to that in the other spectra. Since its intensity appeared constant up to at least 450°C , its presence should not affect the detailed balance arguments for the other spectra in this range. However, the accuracy of the intensity measurements on this broad line is not very good, and if it were due to Mn^{++} , some of the increase in spectrum II could have been produced by an undetected decrease in the intensity of this line. In other words, if this arises from Mn^{++} in some precipitated state, it may act as a source of Mn^{++} ions at

higher temperature, and the assumption of constant concentration would not be valid.

The present result lends support to the assumption that simple association theory is applicable in these solids. The binding energy of approximately 0.4 ev agrees with theoretical estimates.²⁻⁴ It is planned to repeat this experiment on samples of higher purity and of varying concentrations of Mn^{++} . Ionic conductivity measurements will also be performed on these samples, and the results will be reported in a subsequent paper.

VIII. SUMMARY

A detailed study has been made of the Mn^{++} spectrum in NaCl. Five different environments have been identified for the ion. At room temperature, most of the Mn^{++} is not in solution but is in some type of aggregated state. At elevated temperatures, or after quenching, the manganese is dissolved into the lattice, substituting for Na^+ ions. Some of these ions are isolated in the lattice; others are paired off with positive-ion vacancies. A smaller fraction are paired off with a chemical impurity which has not been identified. Both nearest and next-nearest vacancy- Mn^{++} pairs have been observed, and their binding energies are almost equal. By studying the relative number of bound and unbound ions *vs* temperature, the binding energy of the nearest pair can be estimated to be ~ 0.4 ev.

The vacancy pairs were also studied for Mn^{++} in LiCl and KCl. Here again the nearest and next-nearest vacancy sites are approximately equally stable.

The crystalline field theory developed by Watanabe is successful in explaining the fine structure produced by the vacancy and impurity complexes only if the values of the crystalline field are taken to be approximately ten times that estimated on a simple ionic point-charge model. This is interpreted as a failure of the point-charge model, the larger fields arising from charge cloud overlap forces and/or covalency. Differences in the fine structure for the three alkali chlorides indicate the importance of these effects.

ACKNOWLEDGMENTS

The author wishes to acknowledge the substantial contribution of Dr. R. M. Walker in the early stages of this investigation. Thanks also go to Dr. P. D. Johnson for supplying several of the crystals and making his crystal growing apparatus available to us. The author would also like to acknowledge the contributions of Mr. Walter Colliton, who grew several of the crystals and assisted in some of the measurements. Finally, I would like to thank Dr. J. R. Eshbach and Dr. G. W. Ludwig for helpful suggestions concerning the manuscript.

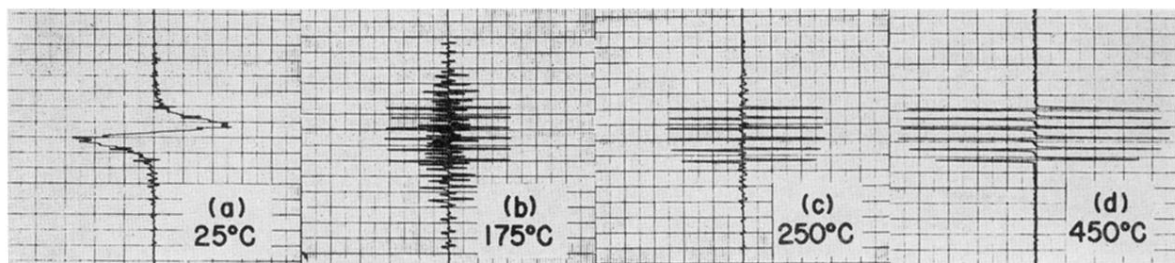


FIG. 3. Spectrum of NaCl:Mn *vs* temperature. The magnetic field is parallel to a cubic axis.